Mathematical Biosciences and Engineering

http://www.aimspress.com/journal/MBE

MBE, 18(5): 6216–6238.
DOI: 10.3934/mbe.2021311
Received: 17 May 2021
Accepted: 13 July 2021
Published: 19 July 2021

Research article

Extracted features of national and continental daily biweekly growth rates of confirmed COVID-19 cases and deaths via Fourier analysis

Ray-Ming Chen*

Department of Mathematics and Statistics, Baise University, 21 Zhongshan No. 2 Road, Basie 533000, China

* **Correspondence:** Email: raymingchen@bsuc.cn.

Abstract: *Aims*: By associating features with orthonormal bases, we analyse the values of the extracted features for the daily biweekly growth rates of COVID-19 confirmed cases and deaths on national and continental levels. *Methods*: By adopting the concept of Fourier coefficients, we analyse the inner products with respect to temporal and spatial frequencies on national and continental levels. The input data are the global time series data with 117 countries over 109 days on a national level; and 6 continents over 447 days on a continental level. Next, we calculate the Euclidean distance matrices and their average variabilities, which measure the average discrepancy between one feature vector and all others. Then we analyse the temporal and spatial variabilities on a national level. By calculating the temporal inner products on a continental level, we derive and analyse the similarities between the continents. *Results*: On the national level, the daily biweekly growth rates bear higher similarities in the time dimension than the ones in the space dimension. Furthermore, there exists a strong concurrency between the features for biweekly growth rates of cases and deaths. As far as the trends of the features are concerned, the features are stabler on the continental level, and less predictive on the national level. In addition, there are very high similarities between all the continents, except Asia. *Conclusions*: The features for daily biweekly growth rates of cases and deaths are extracted via orthonormal frequencies. By tracking the inner products for the input data and the orthonormal features, we could decompose the evolutionary results of COVID-19 into some fundamental frequencies. Though the frequency-based techniques are applied, the interpretation of the features should resort to other methods. By analysing the spectrum of the frequencies, we reveal hidden patterns of the COVID-19 pandemic. This would provide some preliminary research merits for further insightful investigations. It could also be used to predict future trends of daily biweekly growth rates of COVID-19 cases and deaths.

Keywords: COVID-19; biweekly growth rates; variability; Fourier analysis; temporal and spatial

1. Introduction

Since the emergence of the COVID-19 pandemic around December 2019, the outbreak has snowballed globally [1, 2], and there is no clear sign that the new confirmed cases and deaths are coming to an end. Though vaccines are rolling out to deter the spread of this pandemic, the mutations of the viruses are already under way [3–6]. Despite the fact and research that the origin of the pandemic is still in debate [7], many researchers are conducting their study from different aspects and perspectives. They could be categorised mainly into three levels: SARS-CoV-2 genetic level [8], COVID-19 individual country level [9–11] and continental levels [12, 13]. In this study, we focus on the latter two levels. Regarding these two levels, there are many methods and techniques on these issues. For example, linear and non-linear growth models, together with 2-week-kernel-window regression, are exploited in modelling the exponential growth rate of COVID-19 confirmed cases [14] - which are also generalised to non-linear modelling of COVID-19 pandemic [15, 16]. Some research works focus on the prediction of COVID-19 spread by estimating the lead-lag effects between different countries via time warping technique [17], while some utilise clustering analyses to group countries via epidemiological data of active cases, active cases per population, etc. [18]. In addition, there are other researches focusing on tackling the relationship between economic variables and COVID-19 related variables [19, 20] - though both the results show there are no relation between economic freedom and COVID-19 deaths and no relation between the performance of equality markets and the COVID-19 cases and deaths.

In this study, we aim to extract the features of daily biweekly growth rates of cases and deaths on national and continental levels. We devise the orthonormal bases based on Fourier analysis [21, 22], in particular Fourier coefficients for the potential features. For the national levels, we import the global time series data and sample 117 countries for 109 days [23, 24]. Then we calculate the Euclidean distance matrices for the inner products between countries and between days. Based on the distance matrices, we then calculate their variabilities to delve into the distribution of the data. For the continental level, we also import the biweekly changes of cases and deaths for 5 continents as well as the world data with time series data for 447 days. Then we calculate their inner products with respect to the temporal frequencies and find the similarities of extracted features between continents.

For the national levels, the biweekly data bear higher temporal features than spatial features, i..e., as time goes by, the pandemic evolves more in the time dimension than the space (or country-wise) dimension. Moreover, there exists a strong concurrency between features for biweekly changes of cases and deaths, though there is no clear or stable trend for the extracted features. However, in the continental level, one observes that there is a stable trend of features regarding biweekly change. In addition, the extracted features between continents are similar to one another, except Asia whose features bear no clear similarities with other continents.

Our approach is based on orthonormal bases, which serve as the potential features for the biweekly change of cases and deaths. This method is straightforward and easy to comprehend. The limitations of this approach are the extracted features are based on the hidden frequencies of the dynamical structure, which is hard to assign a interpretable meaning for the frequencies, and the data fetched are not complete, due to the missing data in the database. However the results provided in this study could help one map out the evolutionary features of COVID-19.

2. Method and implementation

Let $\delta : \mathbb{N} \to \{0, 1\}$ be a function such that $\delta(n) = 0$ (or $\delta_n = 0$), if $n \in 2\mathbb{N}$ and $\delta(n) = 1$, if $n \in 2\mathbb{N} + 1$. Given a set of point data $\mathbb{D} = \{\vec{v}\} \subseteq \mathbb{R}^N$, we would like to decompose each $\vec{v}$ into some frequency-based vectors by Fourier analysis. The features of COVID-19 case and death growth rates are specified by the orthogonal frequency vectors $\mathbb{B}_N = \{\vec{f_j^i} : 1 \leq j \leq N\}_{i=1}^N$, which is based on Fourier analysis, in particular Fourier series [22], where

- $\vec{f_j^1} = \sqrt{\frac{1}{N}}$ for all $1 \leq j \leq N$;
- For any $2 \leq i \leq N - 1 + \delta_N$,

$$\vec{f_j^i} = \sqrt{\frac{2}{N}} \cdot cos[\frac{\pi}{2} \cdot \delta_i - \frac{(i - \delta_i) \cdot \pi}{N} \cdot j; \tag{2.1}$$

- If $N \in 2\mathbb{N}$, then $\vec{f_j^N} = \sqrt{\frac{1}{N}} \cdot cos(j \cdot \pi)$ for all $1 \leq j \leq N$.

Now we have constructed an orthonormal basis $\mathcal{F}^N = \{\vec{f^1}, \vec{f^2}, \cdots, \vec{f^N}\}$ as features for $\mathbb{R}^N$. Now each $\vec{v} = \sum_{i=1}^{N} < \vec{v}, \vec{f^i} > \cdot \vec{f^i}$, where $<,>$ is the inner product. The basis $\mathbb{B}_N$ could also be represented by a matrix

$$\mathcal{F}^N = \begin{bmatrix} \vec{f^1} \\ \vec{f^2} \\ \vdots \\ \vec{f^N} \end{bmatrix} = \begin{bmatrix} \vec{f_1^1} & \vec{f_2^1} & \cdots & \vec{f_N^1} \\ \vec{f_1^2} & \vec{f_2^2} & \cdots & \vec{f_N^2} \\ \vdots & \vdots & \vdots & \vdots \\ \vec{f_1^N} & \vec{f_2^N} & \cdots & \vec{f_N^N} \end{bmatrix}. \tag{2.2}$$

where each $\vec{f_j^i}$ is defined in Eq 2.1.

Example 1. *If N is 5, then the matrix representation of the orthonormal basis $\mathbb{B}_5$ is*

$$\mathcal{F}^5 = \begin{bmatrix} \vec{f^1} \\ \vec{f^2} \\ \vec{f^3} \\ \vec{f^4} \\ \vec{f^5} \end{bmatrix} = \begin{bmatrix} 0.447 & 0.447 & 0.447 & 0.447 & 0.447 \\ 0.195 & -0.512 & -0.512 & 0.195 & 0.632 \\ 0.602 & 0.372 & -0.372 & -0.602 & 0 \\ -0.512 & 0.195 & 0.195 & -0.512 & 0.632 \\ 0.372 & -0.602 & 0.602 & -0.372 & 0 \end{bmatrix}.$$

and the representation of a data column vector $\vec{v}$ = {(-3, 14, 5, 8,-12)} with respect to $\mathbb{B}_5$ is calculated by $\mathcal{F}^5\vec{v} = [< \vec{v}, \vec{f_i} >]_{i=1}^5$ or a column vector or 5-by-1 matrix (5.367,-16.334,-3.271,-6.434,-9.503).

2.1. Data description and handling

There are two main parts of data collection and handling - one for individual countries (or national level) and the other for individual continents (or continental level). In both levels, we fetch the daily biweekly growth rates of confirmed COVID-19 cases and deaths from Our World in Data [23, 24]. Then we use R programming 4.1.0 to handle the data and implement the procedures.

Sampled targets: national. After filtering out non-essential data and missing data, the effective sampled data are 117 countries with effective sampled 109 days as shown in Results. The days range from December 2020 to June 2021. Though the sampled days are not subsequent ones (due to the missing data), the biweekly information could still cover such loss. In the latter temporal and spatial analyses, we will conduct our study based on these data.

Sampled targets: continental. As for the continental data, we collect data regarding the world, Africa, Asia, Europe, North and South America. The sampled days range from March 22nd, 2020 to June 11th, 2021. In total, there are 449 days (this is different from the national level). In the latter temporal analysis (there is no spatial analysis in the continental level, due to the limited sampling size), we will conduct our study based on these data.

Notations: national. For further processing, let us utilise some notations to facilitate the introduction. Let the sampled countries be indexed by $i = 1, ..., 117$. Let the sampled days be indexed by $t = 1, ..., 109$. Days range from December 3rd 2020 to May 31st 2021. Let $c_i(t)$ and $d_i(t)$ be the daily biweekly growth rates of confirmed cases and deaths in country i on day t, respectively, i.e.,

$$c_i(t) := \frac{case_{i,t+13} - case_{i,t}}{case_{i,t}}; \tag{2.3}$$

$$d_i(t) := \frac{death_{i,t+13} - death_{i,t}}{death_{i,t}}, \tag{2.4}$$

where $case_{i,t}$ and $death_{i,t}$ denote the total confirmed cases and deaths for country i at day t, respectively. We form temporal and spatial vectors by

$$c_i = (c_i(1), ..., c_i(109)); d_i = (d_i(1), ..., d_i(109))$$

$$v(t) = (c_1(t), c_2(t)..., c_{117}(t)); w(t) = (d_1(t), d_2(t)..., d_{117}(t))$$

the vector c_i and d_i give every count in time for a given country, and the vector $v(t)$ and $w(t)$ give every countries' count for a given time.

Notations: continental. For further processing, let us utilise some notations to facilitate the introduction. Let the sampled continents be indexed by $j = 1, ..., 6$. Let the 447 sampled days range from March 22nd 2020 to June 11th 2021. We form temporal vectors for confirmed cases and deaths by

$$x_j = (c_j(1), c_j(2), ..., c_j(447)); y_i = (d_j(1), d_j(2), ..., d_j(447)).$$

2.2. Implementation

For any m-by-n matrix A, we use $min(A)$ to denote the value $min\{a_{ij} : 1 \le i \le m; 1 \le j \le n\}$. Similarly, we define $max(A)$ by the same manner. If $\vec{v}$ is a vector, we define $min(\vec{v})$ and $max(\vec{v})$ in the same manner. The implementation goes as follows:

(1) Extract and trim and source data.
Extraction: national. Extract the daily biweekly growth rates of COVID-19 cases and deaths from the database and trim the data. The trimmed data consist of 109 time series data for 117 countries as shown in Table 1, which consists of two 117-by-109 matrices:

$$Biweekly\_cases = [c_i(t)]_{i=1:117}^{t=1:109}; Biweekly\_deaths = [d_i(t)]_{i=1:117}^{t=1:109}.$$

Row i in the matrices are regarded as temporal vectors c_i and d_i respectively, and Column t in the matrices are regarded as spatial vectors $v(t)$ and $w(t)$ respectively.

Extraction: continental. As for the continental data, they are collected by two 6-by-447 matrices:

$$Biweekly\_cont\_cases = [x_j(\tau)]_{j=1:6}^{\tau=1:447};$$

$$Biweekly\_cont\_deaths = [y_j(t)]_{j=1:6}^{\tau=1:447}.$$

Table 1. Time series data of 109 daily biweekly growth rates for 117 countries for confirmed cases(upper block) and deaths (lower block).

Date	2020/12/3	2020/12/4	2020/12/5	⋯	2021/5/29	2021/5/30	2021/5/31
label	1	2	3	⋯	107	108	109
1	18.64	11.25	−42.3	⋯	−28.2	0.72	58.99
2	3.6	8.73	−40.35	⋯	−28.25	4.58	73.84
3	4.01	4.44	−37.79	⋯	−27.62	3.88	94.77
⋮	⋮	⋮	⋮	⋯	⋮	⋮	⋮
115	12.55	−46.42	31.97	⋯	−7.82	21.65	28.91
116	12.04	−45.49	27.99	⋯	−5.36	41.76	37.63
117	11.42	−43.95	26.28	⋯	−3.47	51.09	39.43
Date	2020/12/3	2020/12/4	2020/12/5	⋯	2021/5/29	2021/5/30	2021/5/31
label	1	2	3	⋯	107	108	109
1	101.04	24.1	−30.54	⋯	−6.41	−9.93	55.56
2	65.14	−1.01	−27.75	⋯	−6.79	−12.12	44.44
3	56.3	−9.31	−29.03	⋯	−7.74	−14.54	40
⋮	⋮	⋮	⋮	⋯	⋮	⋮	⋮
115	28.85	−35.65	−23.24	⋯	−9.8	−9.09	−14.29
116	35.95	−36.89	−23.75	⋯	−9.06	−16.67	0
117	36.77	−33.49	−24.35	⋯	−8.65	0	33.33

(2) Specify the frequencies (features) for the imported data.

Basis: national. In order to decompose c_i and d_i into some fundamental features, we specify $\mathcal{F}^{109}$ as the corresponding features, whereas to decompose $v(t)$ and $w(t)$, we specify $\mathcal{F}^{117}$ as the corresponding features. The results are presented in Table 2.

Basis: continental. In order to decompose x_j and y_j into some fundamental features, we specify $\mathcal{F}^{447}$ as the corresponding features.

(3) Compute the sets of the representations with respect to various bases.

Representation: national. The temporal representations of of c_i and d_i with respect to $\mathcal{F}^{109}$ are calculated by

$$IP\_cases\_time = \{\mathcal{F}^{109}c_i\}_{i=1}^{117},$$

$$IP\_death\_time = \{\mathcal{F}^{109} d_i\}_{i=1}^{117};$$

and the spatial representations of $v(t)$ and $w(t)$ with respect to $\mathcal{F}^{117}$ are calculated by

$$IP\_cases\_space = \{\mathcal{F}^{117} v(t)\}_{t=1}^{109},$$

$$IP\_death\_space = \{\mathcal{F}^{117} w(t)\}_{t=1}^{109}.$$

The results are presented Results.

Representation: continental. The temporal representations of of x_j and y_j with respect to $\mathcal{F}^{447}$ are calculated by

$$IP\_cont\_cases\_time = \{\mathcal{F}^{447} x_j\}_{j=1}^{447},$$

$$IP\_cont\_death\_time = \{\mathcal{F}^{447} y_j\}_{j=1}^{447}.$$

(4) Compute the Euclidean distance matrices for the representations.

Euclidean: national. The distances between temporal representations with respect to cases and deaths by calculated by

$$dismat\_case\_time = [d_E(\mathcal{F}^{109} c_i, \mathcal{F}^{109} c_j)]_{i,j=1}^{117}$$

$$dismat\_death\_time = [d_E(\mathcal{F}^{109} d_i, \mathcal{F}^{109} d_j)]_{i,j=1}^{117};$$

The distances between spatial representations with respect to cases and deaths by calculated by

$$dismat\_case\_space[d_E(\mathcal{F}^{117} v(t), \mathcal{F}^{117} v(\tau))]_{t,\tau=1}^{109}$$

$$dismat\_death\_space = [d_E(\mathcal{F}^{117} w(t), \mathcal{F}^{117} w(\tau))]_{t,\tau=1}^{109},$$

where d_E is the usual Euclidean distance function. The results are presented in Results

Euclidean: continental. The distances between temporal representations with respect to cases and deaths by calculated by

$$dismat\_cont\_case\_time = [d_E(\mathcal{F}^{447} x_j, \mathcal{F}^{447} x_k)]_{j,k=1}^{447}$$

$$dismat\_cont\_death\_time = [d_E(\mathcal{F}^{447} y_j, \mathcal{F}^{447} y_k)]_{j,k=1}^{447}.$$

(5) Compute the average variability based on the above distance matrices.

Average variability: national. For each country i, the temporal variabilities for confirmed cases and deaths are computed by

$$var\_case\_time[i] = \frac{\sum_{j=1}^{117} d_E(\mathcal{F}^{109} c_i, \mathcal{F}^{109} c_j)}{109};$$

$$var\_death\_time[i] = \frac{\sum_{j=1}^{117} d_E(\mathcal{F}^{109} c_i, \mathcal{F}^{109} c_j)}{109};$$

and for each day t, the spatial variabilities for confirmed cases and deaths are computed by

$$var\_case\_space[t] = \frac{\sum_{\tau=1}^{109} d_E(\mathcal{F}^{117}v(t), \mathcal{F}^{117}v(\tau))}{117};$$

$$var\_death\_space[t] = \frac{\sum_{\tau=1}^{109} d_E(\mathcal{F}^{117}w(t), \mathcal{F}^{117}w(\tau))}{117}.$$

The results are presented in Results.

Average variability: continental. For each continent j, the temporal variabilities for confirmed cases and deaths are computed by

$$var\_cont\_case\_time[j] = \frac{\sum_{k=1}^{6} d_E(\mathcal{F}^{447}x_j, \mathcal{F}^{447}x_k)}{447};$$

$$var\_cont\_death\_time[j] = \frac{\sum_{k=1}^{6} d_E(\mathcal{F}^{447}y_j, \mathcal{F}^{447}y_k)}{447}.$$

(6) Unify the national temporal and spatial variabilities of cases and deaths. For each country i, the unified temporal and spatial variabilities for cases and deaths are defined by

- $bvar\_case\_time[i] = \frac{var\_case\_time[i]-mn1}{mx1-mn1}$;
- $bvar\_death\_time[i] = \frac{var\_death\_time[i]-mn2}{mx2-mn2}$;
- $bvar\_case\_space[t] = \frac{var\_case\_space[t]-mn3}{mx3-mn3}$;
- $bvar\_death\_space[t] = \frac{var\_death\_space[t]-mn4}{mx4-mn4}$,

where

- $mn1 = min(var\_case\_time); mx1 = max(var\_case\_time)$;
- $mn2 = min(var\_death\_time); mx2 = max(var\_death\_time)$;
- $mn3 = min(var\_case\_space); mx3 = max(var\_case\_space)$;
- $mn4 = min(var\_death\_space); mx4 = max(var\_death\_space)$. The results are shown in Results.

(7) Unified temporal representations with respect to continental confirmed cases and deaths by matrices whose (i, j) cell are defined by

$$\frac{\sigma_{ij} - min(IP\_cont\_cases\_time)}{max(IP\_cont\_cases\_time) - min(IP\_cont\_cases\_time)};$$

$$\frac{\beta_{ij} - min(IP\_cont\_death\_time)}{max(IP\_cont\_death\_time) - min(IP\_cont\_death\_time)};$$

where σ_{ij} and β_{ij} denotes the value in the (i, j) cells of $IP\_cont\_cases\_time$ and $IP\_cont\_deaths\_time$, respectively. The results are visualised by figures in Results.

3. Results

There are two main parts of results shown in this section: national results and continental results.

National results. Based on the method mentioned in section 2, we identify the temporal orthonormal frequencies and spatial ones as shown in Table 2.

Table 2. Orthonormal temporal frequencies for 109 days (upper block or $\mathcal{F}^{109}$) and orthonormal spatial frequencies for 117 countries (lower block or $\mathcal{F}^{117}$).

temp. freq.	ele. 1	ele. 2	ele. 3	$\cdots$	ele. 107	ele. 108	ele. 109
$\vec{f}^1$	0.1	0.1	0.1	$\cdots$	0.1	0.1	0.1
$\vec{f}^2$	0.14	0.13	0.13	$\cdots$	0.13	0.14	0.14
$\vec{f}^3$	0.01	0.02	0.02	$\cdots$	−0.02	−0.01	0
$\vdots$	$\vdots$	$\vdots$	$\vdots$	$\cdots$	$\vdots$	$\vdots$	$\vdots$
$\vec{f}^{107}$	0.01	−0.02	0.03	$\cdots$	0.02	−0.01	0
$\vec{f}^{108}$	−0.14	0.14	−0.13	$\cdots$	0.14	−0.14	0.14
$\vec{f}^{109}$	0	−0.01	0.01	$\cdots$	0.01	0	0
spatial. freq.	ele. 1	ele. 2	ele. 3	$\cdots$	ele. 115	ele. 116	ele. 117
$\vec{f}^1$	0.09	0.09	0.09	$\cdots$	0.09	0.09	0.09
$\vec{f}^2$	0.13	0.13	0.13	$\cdots$	0.13	0.13	0.13
$\vec{f}^3$	0.01	0.01	0.02	$\cdots$	−0.01	−0.01	0
$\vdots$	$\vdots$	$\vdots$	$\vdots$	$\cdots$	$\vdots$	$\vdots$	$\vdots$
$\vec{f}^{115}$	0.01	-0.02	0.03	$\cdots$	0.02	−0.01	0
$\vec{f}^{116}$	−0.13	0.13	−0.13	$\cdots$	0.13	−0.13	0.13
$\vec{f}^{117}$	0	−0.01	0.01	$\cdot$	0.01	0	0

The computed inner products at country levels, served as the values for extracted features, for daily biweekly growth rates of cases and deaths with respect to temporal frequencies are shown in Figure 1. Similarly, the computed inner products at a country level for daily biweekly growth rates of cases and deaths with respect to spatial frequencies are shown in Figure 2. Meanwhile, their scaled variabilities are plotted in Figure 3.

Continental results. According to the obtained data, we study and compare continental features of daily biweekly growth rates of confirmed cases and deaths of Africa, Asia, Europe, North America, South America and World. Unlike the missing data in analysing individual countries, the continental data are complete. We take the samples from March 22nd, 2020 to June 11th, 2021. In total, there are 447 days for the analysis. The cosine values which compute the similarities between representations for continents are shown in Table 3. The results of the unified inner products with respect to confirmed cases and deaths are plotted in Figures 4 and 5, respectively.

Other auxiliary results that support the plotting of the graphs are also appended in Appendix. The names of the sampled 117 countries are provided in Tables A1 and A2. The dates of the sampled days are provided in Figure A1. The tabulated results for inner product of temporal and spatial frequencies on a national level are provided in Table A3. The tabulated results for inner product of temporal

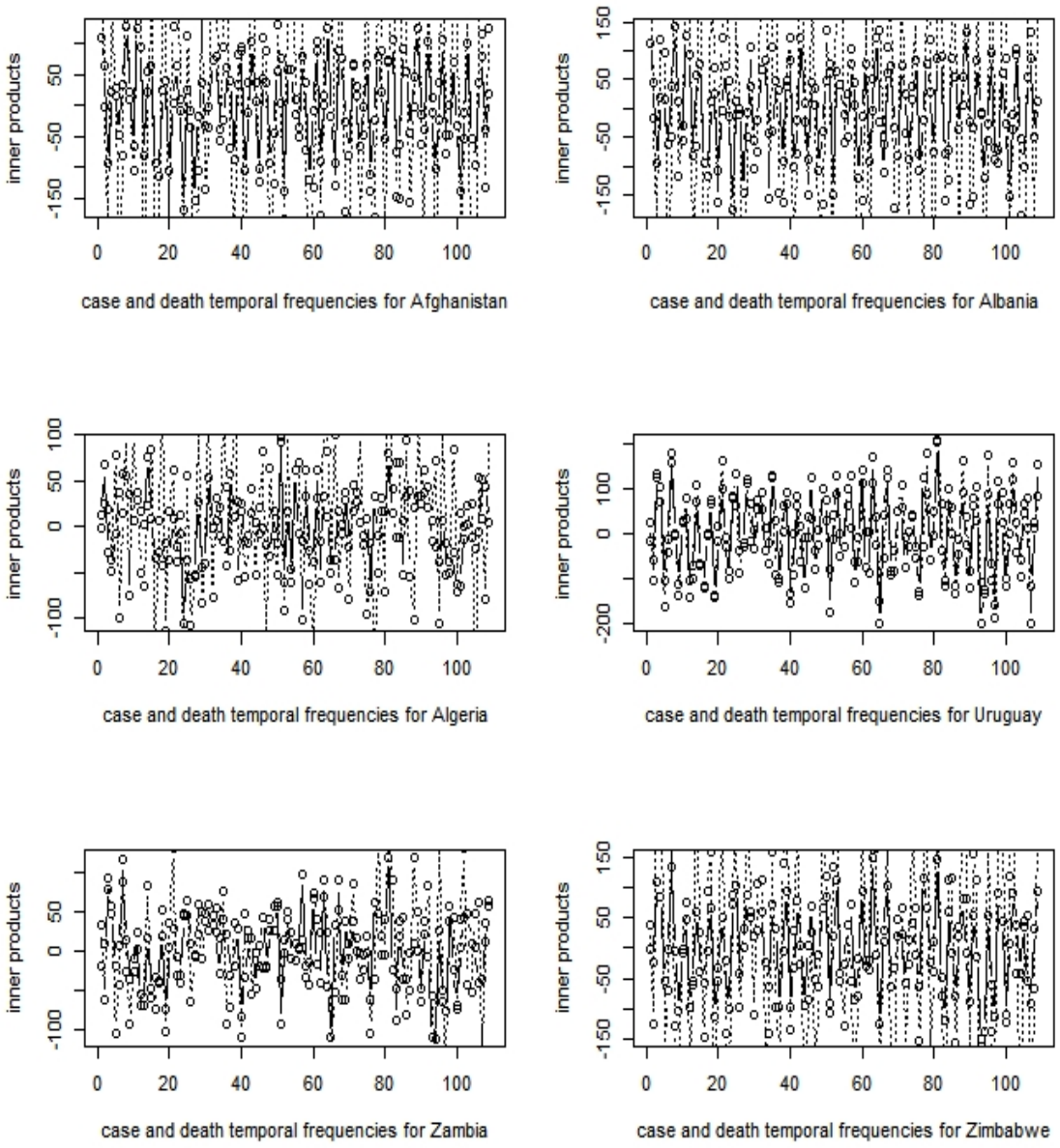

;

Figure 1. Inner products between growth rates of cases (in solid line) over 109 temporal frequencies; and inner products between growth rates of deaths (in dotted line) over 109 temporal frequencies for some demonstrative countries: Afghanistan, Albania, Algeria, Uruguay, Zambia, and Zimbabwe.

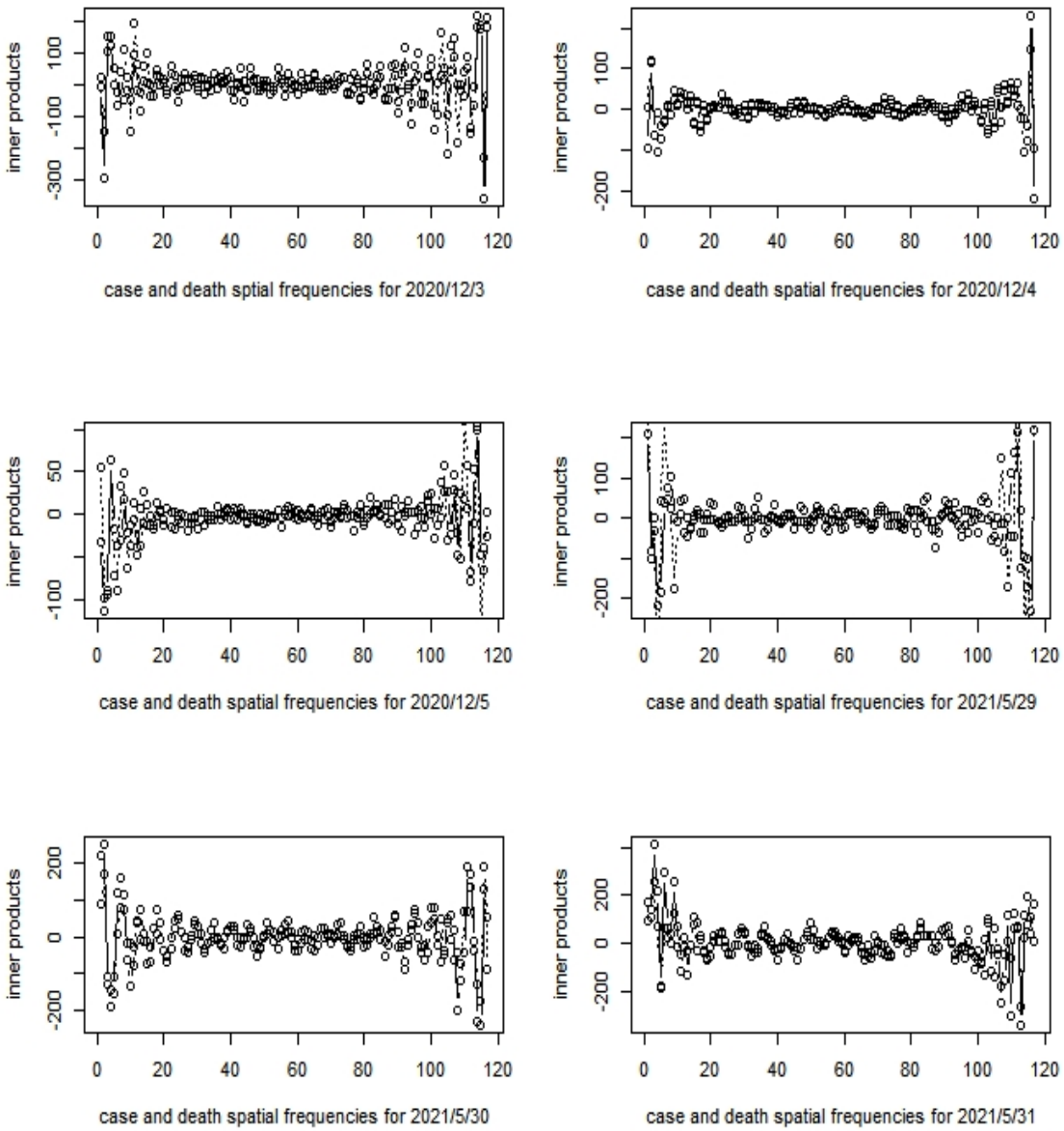

;

Figure 2. Inner products between growth rates of cases (in solid line) over 117 spatial frequencies; and inner products between growth rates of deaths (in dotted line) over 117 spatial frequencies for some demonstrative dates: 2020/12/3, 2020/12/4, 2020/12/5, 2021/5/29, 2021/5/30, and 2021/5/31.

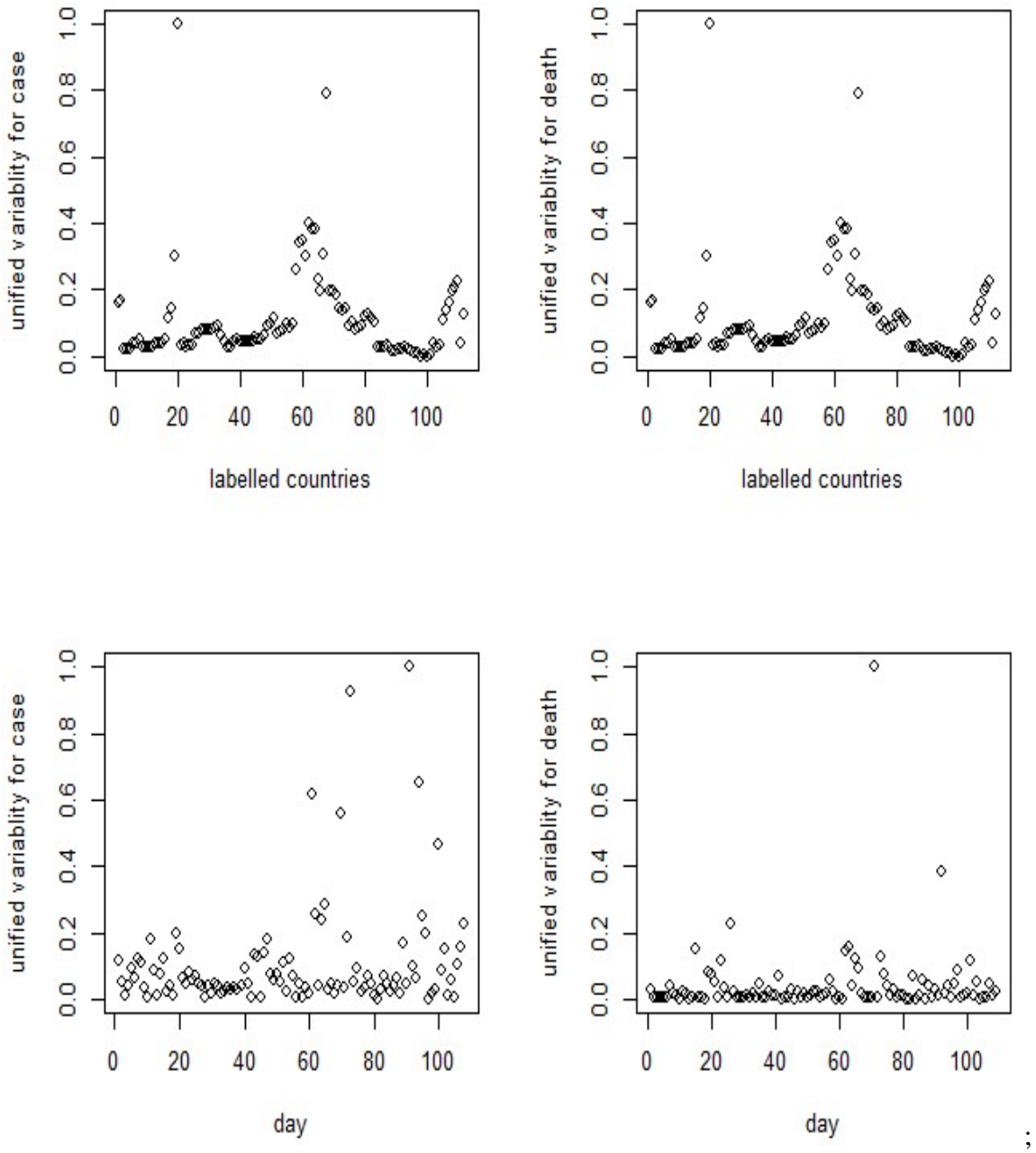

;

Figure 3. Unified temporal and spatial variabilities of daily biweekly growth rates of cases and deaths.

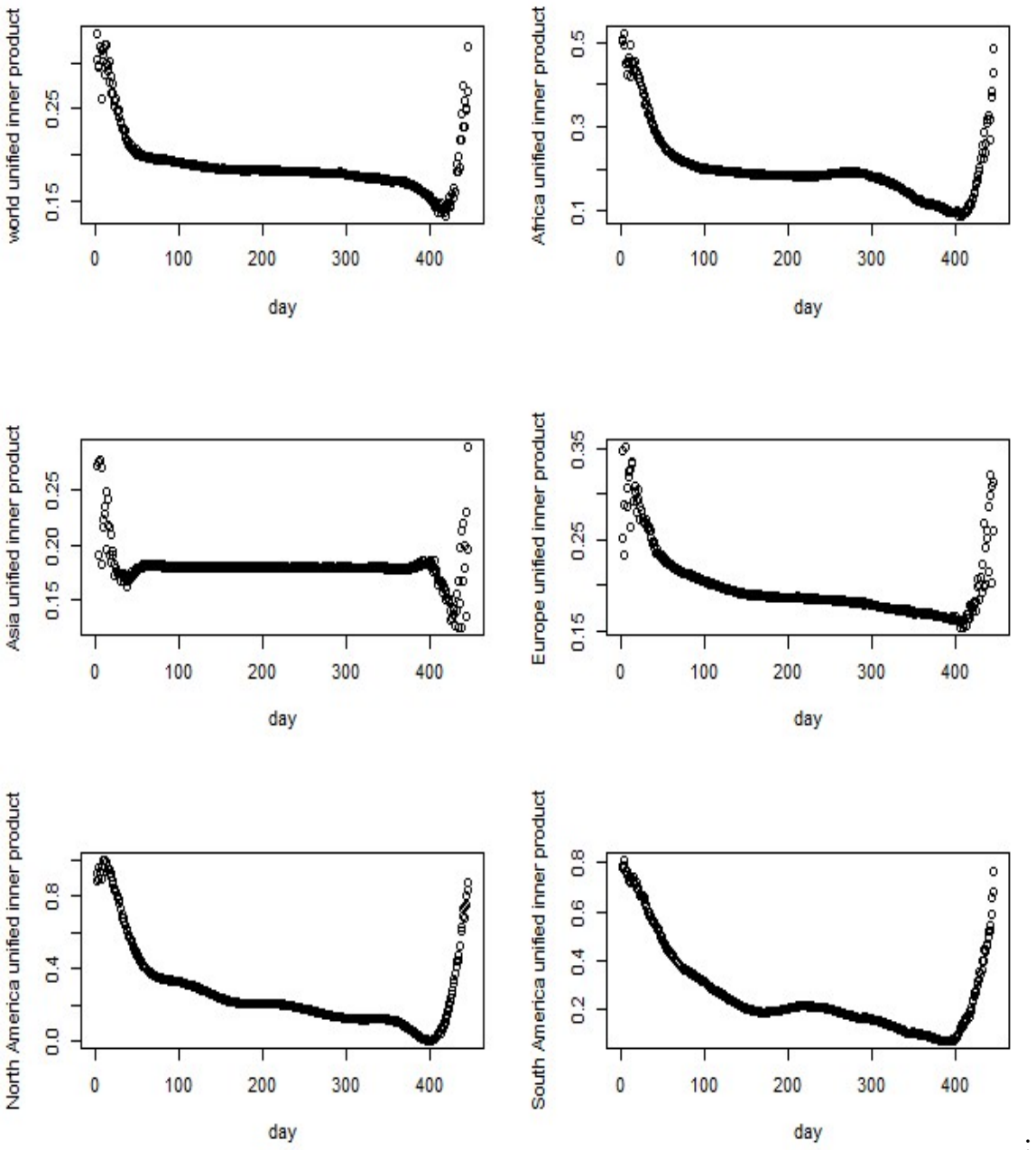

;

Figure 4. Unified inner product, or UIP, for World, Africa, Asia, Europe, North and South America with respect to biweekly growth rates of cases.

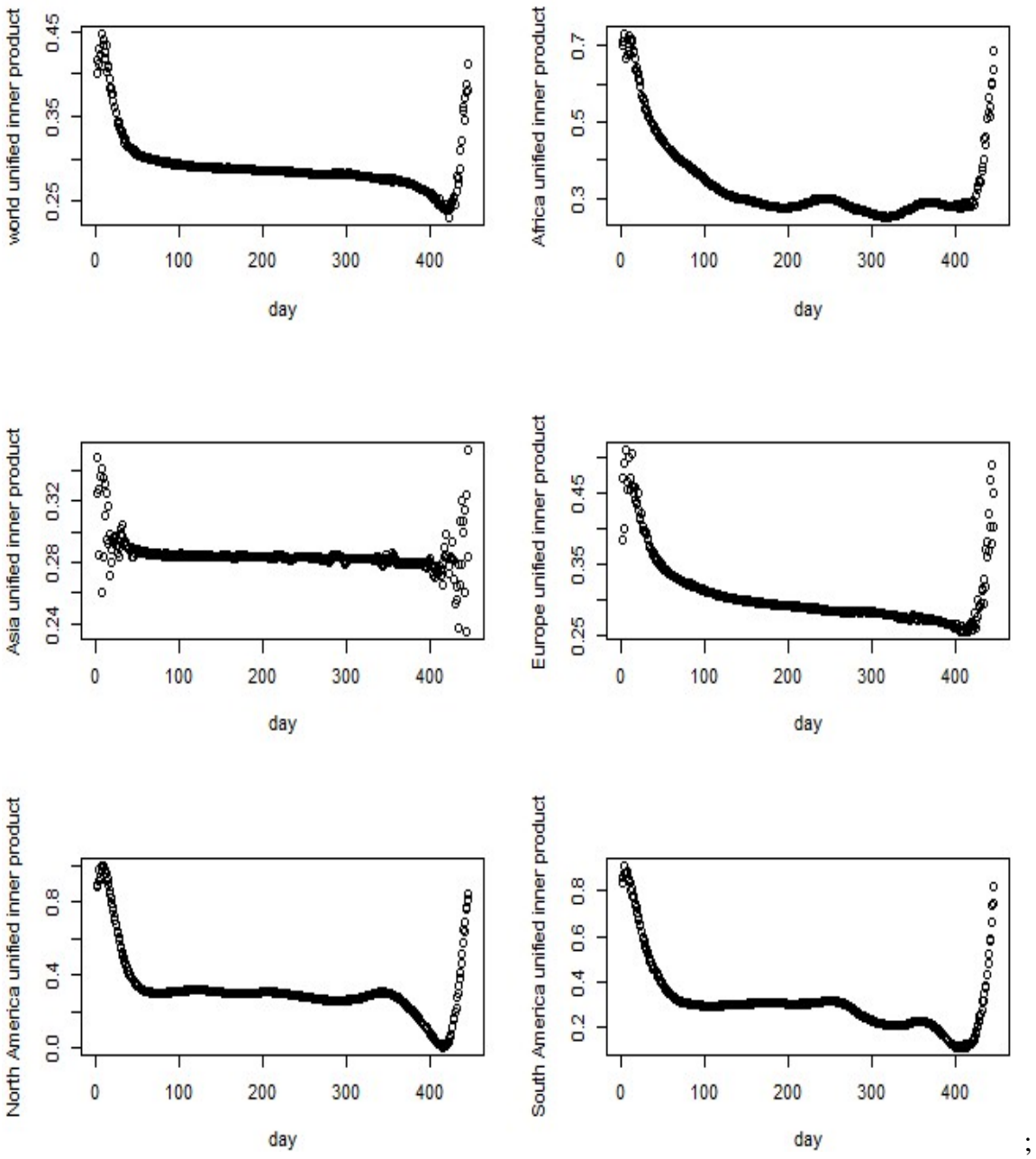

Figure 5. Unified inner product, or UIP, for world, Africa, Asia, Europe, North and South America with respect to daily biweekly growth rates of deaths.

Table 3. Cosine values (similarities) between World, Africa, Asia, Europe, North America (No. Am.), and South America (So. Am.).

	World	Africa	Asia	Europe	No. Am.	So. Am.
World	1.000	0.963	0.638	0.923	0.938	0.890
Africa	0.963	1.000	0.484	0.926	0.965	0.941
Asia	0.638	0.484	1.000	0.391	0.399	0.356
Europe	0.923	0.926	0.391	1.000	0.968	0.956
No. Am.	0.938	0.965	0.399	0.968	1.000	0.983
So. Am.	0.890	0.941	0.356	0.956	0.983	1.000
	World	Africa	Asia	Europe	No. Am.	So. Am.
World	1.000	0.895	0.647	0.936	0.978	0.972
Africa	0.895	1.000	0.553	0.966	0.843	0.891
Asia	0.647	0.553	1.000	0.547	0.596	0.615
Europe	0.936	0.966	0.547	1.000	0.893	0.917
No. Am.	0.978	0.843	0.596	0.893	1.000	0.967
So. Am.	0.972	0.891	0.615	0.917	0.967	1.000

frequencies on a continental level are provided in Table A4. The Euclidean distance matrices for temporal and spatial representations with respect to confirmed cases and deaths are tabulated in Table A5 and their average variabilities are tabulated in Table A6.

Summaries of results. Based on the previous tables and figures, we have the following results.

(1) From Figures 1 and 2, one observes that the temporal features are much more distinct that the spatial features, i.e., if one fixes one day and extracts the features from the spatial frequencies, he obtains less distinct features when comparing with fixing one country and extracting the features from the temporal frequencies. This indicates that SARS-CoV-2 evolves and mutates mainly according to time than space.

(2) For individual countries, the features for the biweekly changes of cases are almost concurrent with those of deaths. This indicates biweekly changes of cases and deaths share the similar features. In some sense, the change of deaths is still in tune with the change of confirmed cases, i.e., there is no substantial change between their relationship.

(3) For individual countries, the extracted features go up and down intermittently and there is no obvious trend. This indicates the virus is still very versatile and hard to capture its fixed features in a country-level.

(4) From Figure 3, one observes that there is a clear similarities, in terms of variabilities, for both daily biweekly growth rates of cases and deaths under temporal frequencies. Moreover, the distribution of overall data is not condensed, where middle, labelled countries are scattering around the whole data. This indicates the diversity of daily biweekly growth rates of cases and deaths across countries is still very high.

(5) From Figure 3, the daily biweekly growth rates of deaths with respect to the spatial frequencies

are fairly concentrated. This indicates the extracted features regarding deaths are stable, i.e., there are clearer and stabler spatial features for daily biweekly growth rates of deaths.

(6) Comparing the individual graphs in Figures 4 and 5, they bear pretty much the same shape, but in different scale - with death being higher feature oriented (this is also witnessed in a country-level as claimed in the first result above). This indicates there is a very clear trend of features regarding daily biweekly growth rates in a continental level (this is a stark contrast to the third claimed result above).

(7) From Figures 4 and 5, the higher values of inner products lie in both endpoints for biweekly change of cases and deaths, i.e., low temporal frequencies and high temporal frequencies for all the continents, except the biweekly change of deaths in Asia. This indicates the evolutionary patterns in Asia are very distinct from other continents.

(8) From Table 3, the extracted features are all very similar to each continents, except Asia. This echoes the above result.

4. Conclusions and future work

In this study, we identify the features of daily biweekly growth rates of COVID-19 confirmed cases and deaths via orthonormal bases (features) which derive from Fourier analysis. Then we analyse the inner products which represent the levels of chosen features. The variabilities for each country show the levels of deaths under spatial frequencies are much more concentrated than others. The generated results are summarised in Results 3. There are some limitations in this study and future improvements to be done:

- The associated meanings of the orthonormal features from Fourier analysis are not yet fully explored;
- We use the Euclidean metric to measure the distances between features, which is then used to calculate the variabilities. Indeed Euclidean metric is noted for its geographical properties, but may not be the most suitable in the context of frequencies. One could further introduce other metrics and apply machine learning techniques to find out the optimal ones.
- In this study, we choose the daily biweekly growth rates of confirmed cases and deaths as our research sources. This is a one-sided story. To obtain a fuller picture of the dynamical features, one could add other variables for comparison.

Acknowledgements

This work is supported by the Humanities and Social Science Research Planning Fund Project under the Ministry of Education of China (No. 20XJAGAT001).

Conflict of interest

No potential conflict of interest was reported by the authors.

References

1. Y. Wu, C. Chen, Y. Chan, The outbreak of COVID-19: An overview, *J. Chin. Med. Assoc.*, **83** (2020), 217–220.
2. C. Huang, Y. Wang, X. Li, L. Ren, J. Zhao, Y. Hu, et al., Clinical features of patients infected with 2019 novel coronavirus in Wuhan, China, *Lancet*, **395** (2020), 497–506.
3. N. Davies, S. Abbott, R. Barnard, C. Jarvis, A. Kucharski, J. Munday, et al., Estimated transmissibility and impact of SARS-CoV-2 lineage B.1.1.7 in England, *Science*, **372** (2021), 497–506.
4. S. Madhi, V. Baillie, C. Cutland, M. Voysey, A. Koen, L. Fairlie, et al., Efficacy of the ChAdOx1 nCoV-19 Covid-19 Vaccine against the B.1.351 Variant, *N. Engl. J. Med.*, **384** (2021), 1885–1898.
5. T. Tada, H. Zhou, B. Dcosta, M. Samanovic, M. Mulligan, N. Landau, The Spike Proteins of SARS-CoV-2 B.1.617 and B.1.618 Variants Identified in India Provide Partial Resistance to Vaccine-elicited and Therapeutic Monoclonal Antibodies, *bioRxiv*, 2021.
6. H. Tegally, E. Wilkinson, M. Giovanetti, A. Iranzadeh, V. Fonseca, J. Giandhari, et al., Detection of a SARS-CoV-2 variant of concern in South Africa, *Nature*, **592** (2001), 438–443.
7. R. Chen, Randomness for Nucleotide Sequences of SARS-CoV-2 and Its Related Subfamilies, *Comput. Math. Methods Med.*, **2020** (2020), 1–8.
8. R. Chen, Distance matrices for nitrogenous bases and amino acids of SARS-CoV-2 via structural metric, *J. Bioinf. Comput. Biol.*, **2021** (2021), 2150011.
9. C. Courtemanche, J. Garuccio, A. Le, J. Pinkston, A. Yelowitz, Strong Social Distancing Measures In The United States Reduced The COVID-19 Growth Rate: Study evaluates the impact of social distancing measures on the growth rate of confirmed COVID-19 cases across the United States, *Health Aff.*, **39** (2020), 1237–1246.
10. R. Chen, On COVID-19 country containment metrics: a new approach, *J. Decis. Syst.*, **2021** (2021), 1–18.
11. R. Chen. Track the dynamical features for mutant variants of COVID-19 in the UK, *Math. Biosci. Eng.*, **18** (2021), 4572–4585.
12. J. Nick, M. Max, R. Peter, COVID-19 second wave mortality in Europe and the United States, *Chaos*, **31** (2021), 031105.
13. M. Cesar, B. Eduardo, S. Rafael, M. Carlos, B. Marcus, Strong correlations between power-law growth of COVID-19 in four continents and the inefficiency of soft quarantine strategies, *Chaos*, **30** (2020), 041102.
14. R. Omori, K. Mizumoto, G. Chowell, Changes in testing rates could mask the novel coronavirus disease (COVID-19) growth rate, *Int. J. Infect. Dis.*, **94** (2020), 116-118.
15. J. Machado, A. Lopes, Rare and extreme events: the case of COVID-19 pandemic, *Nonlinear Dyn.*, **100** (2020), 2953–2972.
16. J. Nick, M. Max, Trends in COVID-19 prevalence and mortality: A year in review, *Phys. D*, **425** (2021), 132968.

17. J. Stübinger, L. Schneider, Epidemiology of coronavirus COVID-19: Forecasting the future incidence in different countries, in *Healthcare*, Multidisciplinary Digital Publishing Institute, **8** (2020), 99.

18. Z. Vasilios, P. G. Stavros, G. Zoe, Z. Efthimios, Clustering analysis of countries using the COVID-19 cases dataset, *Data Brief*, **31** (2020), 105787.

19. R. Chen, Whether Economic Freedom Is Significantly Related to Death of COVID-19, *J. Healthcare Eng.*, **2020** (2020), 1–9.

20. J. Nick, M. Max, Association between COVID-19 cases and international equity indices, *Phys. D*, **417** (2021), 132809.

21. S. L. Arthur, An Introduction to Fourier Analysis. Available from: https://www.math.bgu.ac.il/l̃eonid/ode_9171_files/Schoenstadt_Fourier_PDE.pdf.

22. H. B. Kenneth, *Principles of Fourier Analysis*, CRC Press, 2016.

23. Our World in Data, Biweekly change in confirmed COVID-19 cases, 2021. Available from: https://ourworldindata.org/grapher/biweekly-growth-covid-cases.

24. Our World in Data, Biweekly change in confirmed COVID-19 deaths, 2021. Available from: https://ourworldindata.org/grapher/biweekly-change-covid-death.

Appendix

```
  [1] "2020/12/3"  "2020/12/4"  "2020/12/5"  "2020/12/6"  "2020/12/7"  "2020/12/8"
  [7] "2020/12/9"  "2020/12/10" "2020/12/11" "2020/12/18" "2020/12/19" "2020/12/20"
 [13] "2020/12/21" "2020/12/22" "2020/12/23" "2020/12/24" "2020/12/25" "2020/12/26"
 [19] "2020/12/27" "2020/12/28" "2020/12/29" "2020/12/31" "2021/1/1"   "2021/1/2"
 [25] "2021/1/3"   "2021/1/4"   "2021/1/5"   "2021/2/17"  "2021/2/18"  "2021/2/19"
 [31] "2021/2/20"  "2021/2/21"  "2021/2/22"  "2021/2/23"  "2021/2/24"  "2021/2/25"
 [37] "2021/2/26"  "2021/2/27"  "2021/2/28"  "2021/3/1"   "2021/3/2"   "2021/3/3"
 [43] "2021/3/4"   "2021/3/5"   "2021/3/6"   "2021/3/7"   "2021/3/8"   "2021/3/9"
 [49] "2021/3/10"  "2021/3/11"  "2021/3/12"  "2021/3/13"  "2021/3/14"  "2021/3/15"
 [55] "2021/3/16"  "2021/3/17"  "2021/3/18"  "2021/3/19"  "2021/3/20"  "2021/3/21"
 [61] "2021/3/22"  "2021/3/23"  "2021/4/9"   "2021/4/10"  "2021/4/11"  "2021/4/12"
 [67] "2021/4/13"  "2021/4/14"  "2021/4/15"  "2021/4/16"  "2021/4/17"  "2021/4/18"
 [73] "2021/4/19"  "2021/4/20"  "2021/4/21"  "2021/4/22"  "2021/4/23"  "2021/4/24"
 [79] "2021/4/25"  "2021/4/26"  "2021/4/27"  "2021/5/4"   "2021/5/5"   "2021/5/6"
 [85] "2021/5/7"   "2021/5/8"   "2021/5/9"   "2021/5/10"  "2021/5/11"  "2021/5/12"
 [91] "2021/5/13"  "2021/5/14"  "2021/5/15"  "2021/5/16"  "2021/5/17"  "2021/5/18"
 [97] "2021/5/19"  "2021/5/20"  "2021/5/21"  "2021/5/22"  "2021/5/23"  "2021/5/24"
[103] "2021/5/25"  "2021/5/26"  "2021/5/27"  "2021/5/28"  "2021/5/29"  "2021/5/30"
[109] "2021/5/31"
```

Figure A1. Sampled dates.

Table A1. Country codes: part one.

1	2	3	4
Afghanistan	Albania	Algeria	Argentina
5	6	7	8
Armenia	Austria	Azerbaijan	Bahrain
9	10	11	12
Bangladesh	Belarus	Belgium	Bolivia
13	14	15	16
Bosnia and Herzegovina	Brazil	Bulgaria	Cameroon
17	18	19	20
Canada	Cape Verde	Chile	Colombia
21	22	23	24
Congo	Costa Rica	Cote d'Ivoire	Croatia
25	26	27	28
Cuba	Cyprus	Czechia	Congo
29	30	31	32
Denmark	Dominican Republic	Ecuador	Egypt
33	34	35	36
El Salvador	Estonia	Ethiopia	Finland
37	38	39	40
France	Gabon	Georgia	Germany
41	42	43	44
Ghana	Greece	Guatemala	Guinea
45	46	47	48
Guyana	Honduras	Hungary	India
49	50	51	52
Indonesia	Iran	Iraq	Ireland
53	54	55	56
Israel	Italy	Jamaica	Japan
57	58	59	60
Jordan	Kazakhstan	Kenya	Kosovo

Table A2. Country codes: part two.

61	62	63	64
Kuwait	Kyrgyzstan	Latvia	Lebanon
65	66	67	68
Lithuania	Luxembourg	Madagascar	Malaysia
69	70	71	72
Maldives	Malta	Mauritania	Mexico
73	74	75	76
Moldova	Morocco	Mozambique	Nepal
77	78	79	80
Netherlands	Nicaragua	Niger	Nigeria
81	82	83	84
North Macedonia	Norway	Oman	Pakistan
85	86	87	88
Palestine	Panama	Paraguay	Peru
89	90	91	92
Philippines	Poland	Portugal	Qatar
93	94	95	96
Romania	Russia	Rwanda	Saudi Arabia
97	98	99	100
Senegal	Serbia	Somalia	South Africa
101	102	103	104
South Korea	Spain	Sri Lanka	Sudan
105	106	107	108
Sweden	Switzerland	Syria	Togo
109	110	111	112
Turkey	Uganda	Ukraine	United Arab Emirates
113	114	115	116
United Kingdom	United States	Uruguay	Zambia
117			
Zimbabwe			

Table A3. Inner products w.r.t. temporal (case: upper top and death: upper bottom blocks) and spatial (case: lower top and death: lower bottom blocks) frequencies at a national level.

	1	2	3	⋯	107	108	109
1	110.53	62.66	−93.32	⋯	77.81	−39.04	18.77
2	112.67	46.17	−92.52	⋯	87.26	−47.41	12.92
3	12.98	67.61	−27.31	⋯	51.41	43.11	5.06
⋮	⋮	⋮	⋮	⋯	⋮	⋮	⋮
115	−17.59	−58.27	134.11	⋯	−114.95	23.12	152.09
116	−19.65	8.52	79.69	⋯	−35.33	36.47	65.35
117	−2.64	−22.75	108.62	⋯	−92.29	32.71	94.36
1	366.35	−1.46	−210.92	⋯	116.03	−131.95	126.11
2	326.53	−17.45	−208.92	⋯	133.41	−233.80	208.15
3	−0.74	24.33	18.58	⋯	8.17	−78.58	108.78
⋮	⋮	⋮	⋮	⋯	⋮	⋮	⋮
115	25.84	−105.22	122.77	⋯	−199.31	12.66	82.39
116	32.41	−62.45	92.73	⋯	−137.71	11.78	56.31
117	39.29	−124.70	296.81	⋯	−359.07	−65.38	202.47
	1	2	3	⋯	115	116	117
1	−4.15	−291.26	152.02	⋯	189.07	−356.05	209.52
2	−92.29	115.53	−61.74	⋯	−38.31	228.48	−215.91
3	−31.84	−114.23	−93.34	⋯	−46.84	−65.16	−26.38
⋮	⋮	⋮	⋮	⋯	⋮	⋮	⋮
107	208.69	−103.92	−32.68	⋯	−169.51	−233.38	219.35
108	217.87	251.94	−125.90	⋯	−238.90	130.16	52.03
109	170.73	107.86	416.69	⋯	196.56	40.43	163.64
1	20.39	−145.38	106.48	⋯	174.21	−227.71	182.89
2	4.29	118.47	−61.71	⋯	−78.04	149.29	−94.80
3	56.22	−97.81	−90.43	⋯	−132.01	−38.92	2.25
⋮	⋮	⋮	⋮	⋯	⋮	⋮	⋮
107	285.28	−85.01	−1.29	⋯	−99.33	−401.99	407.84
108	88.85	167.76	−108.55	⋯	−175.93	188.25	−86.94
109	91.87	139.50	262.08	⋯	80.87	111.20	10.58

Table A4. Temporal inner product for continents (World, Africa, Asia, Europe, North and South America) w.r.t. daily biweekly growth rates of cases (upper block) and deaths (lower block) from March 22nd, 2020 to June 11th, 2021 (447 days).

	1	2	3	⋯	445	446	447
World	653.77	686.84	700.11	⋯	−27.98	−27.77	−26.93
Africa	1551.22	1818.89	2003.92	⋯	38.31	43.08	44.42
Asia	51.47	59.75	68.83	⋯	−40.74	−41.06	−41.41
Europe	1234.23	1118.72	1016.35	⋯	−29.31	−28.57	−28.50
North.America	6319.48	7234.23	6924.07	⋯	−31.72	−33.09	−31.97
South.America	5602.78	6116.46	5568.32	⋯	1.87	1.74	4.91
World	731.76	842.64	854.91	⋯	−14.38	−12.32	−11.88
Africa	4600.00	5500.00	3000.00	⋯	5.26	4.38	5.22
Asia	113.03	145.76	157.64	⋯	−24.24	−19.13	−18.54
Europe	1980.05	1806.36	1531.68	⋯	−30.64	−29.34	−28.41
North.America	2823.81	3439.13	3551.72	⋯	21.91	6.88	4.41
South.America	2533.33	3200.00	4200.00	⋯	−2.92	−1.13	−0.67

Table A5. Distance matrices for daily biweekly growth rates of cases (uppermost block) and deaths (2nd block) w.r.t. temporal frequencies and the ones of cases (3rd block) and deaths (bottommost block) w.r.t. spatial frequencies.

	1	2	3	⋯	115	116	117
1	0	106.7561	662.1251	⋯	1228.0185	873.9556	1040.8007
2	106.7561	0	670.5732	⋯	1240.0159	892.0054	1054.962
3	662.1251	670.5732	0	⋯	1040.3623	585.0852	813.6218
⋮	⋮	⋮	⋮	⋯	⋮	⋮	⋮
115	1228.0185	1240.0159	1040.3623	⋯	0	607.239	340.4118
116	873.9556	892.0054	585.0852	⋯	607.239	0	386.7496
117	1040.8007	1054.962	813.6218	⋯	340.4118	386.7496	0
1	0	701.2076	1977.59	⋯	2120.7301	2032.9264	2635.872
2	701.2076	0	2043.929	⋯	2342.249	2269.9992	2802.319
3	1977.5901	2043.9292	0	⋯	1178.0557	1054.5304	1942.125
⋮	⋮	⋮	⋮	⋯	⋮	⋮	⋮
115	2120.7301	2342.249	1178.056	⋯	0	328.4664	1126.271
116	2032.9264	2269.9992	1054.53	⋯	328.4664	0	1355.298
117	2635.8716	2802.3189	1942.125	⋯	1126.2709	1355.2977	0
	1	2	3	⋯	107	108	109
1	0	1001.7219	655.3515	⋯	898.4473	1291.1967	1139.945
2	1001.7219	0	524.0962	⋯	903.7544	848.0297	1166.972
3	655.3515	524.0962	0	⋯	717.0677	908.4058	1151.471
⋮	⋮	⋮	⋮	⋯	⋮	⋮	⋮
107	898.4473	903.7544	717.0677	⋯	0	778.5017	1172.124
108	1291.1967	848.0297	908.4058	⋯	778.5017	0	1297.228
109	1139.9453	1166.9716	1151.4709	⋯	1172.1237	1297.2278	0
1	0	1013.4563	770.5213	⋯	1382.64	1138.3808	1099.3026
2	1013.4563	0	519.0499	⋯	1168.676	418.6043	776.2315
3	770.5213	519.0499	0	⋯	1206.915	629.7284	842.2901
⋮	⋮	⋮	⋮	⋯	⋮	⋮	⋮
107	1382.6399	1168.6759	1206.915	⋯	0	1158.8305	1369.2354
108	1138.3808	418.6043	629.7284	⋯	1158.83	0	808.8633
109	1099.3026	776.2315	842.2901	⋯	1369.235	808.8633	0

Table A6. Variability for 117 countries with respect to daily biweekly growth rates of cases and death under temporal frequencies and variability for 109 days with respect to daily biweekly growth rates of cases and death under spatial frequencies.

	1	2	3	⋯	115	116	117
var_case_time	1025.64	1037.49	779.02	⋯	1145.40	806.55	965.68
var_death_time	2406.49	2610.72	1546.89	⋯	1582.22	1450.46	2249.04
	1	2	3	⋯	107	108	109
var_case_country	923.10	763.91	657.83	⋯	893.60	1029.93	1204.01
var_death_country	1277.72	1019.70	998.01	⋯	1477.71	1110.46	1216.24

AIMS Press